NeuroImage: Clinical 25 (2020) 102200

Contents lists available at ScienceDirect

NeuroImage: Clinical

journal homepage: www.elsevier.com/locate/ynicl

Correlation of microglial activation with white matter changes in dementia with Lewy bodies

Nicolas Nicastro[a,b,1], Elijah Mak[a,1], Guy B. Williams[c], Ajenthan Surendranathan[a], W Richard Bevan-Jones[d], Luca Passamonti[d,e], Patricia Vàzquez Rodrìguez[d], Li Su[a,f], Robert Arnold[d], Tim D. Fryer[c,d], Young T. Hong[c,d], Franklin I. Aigbirhio[c], James B. Rowe[d,g,2], John T. O'Brien[a,2,*]

[a] Department of Psychiatry, University of Cambridge, UK
[b] Department of Clinical Neurosciences, Geneva University Hospitals, Switzerland
[c] Wolfson Brain Imaging Centre, University of Cambridge, UK
[d] Department of Clinical Neurosciences, University of Cambridge, Cambridge, UK
[e] Consiglio Nazionale delle Ricerche (CNR), Istituto di Bioimmagini e Fisiologia Molecolare (IBFM), Milano, Italy
[f] China-UK Centre for Cognition and Ageing Research, Southwest University, Chongqing, China
[g] Medical Research Council Cognition and Brain Sciences Unit, Cambridge, UK

ARTICLE INFO

Keywords:
Dementia
PET
Neuroinflammation
Diffusion tensor imaging

ABSTRACT

Dementia with Lewy bodies (DLB) is characterized by alpha-synuclein protein deposition with variable degree of concurrent Alzheimer's pathology. Neuroinflammation is also increasingly recognized as a significant contributor to degeneration. We aimed to examine the relationship between microglial activation as measured with [^{11}C]-PK11195 brain PET, MR diffusion tensor imaging (DTI) and grey matter atrophy in DLB. Nineteen clinically probable DLB and 20 similarly aged controls underwent 3T structural MRI (T1-weighted) and diffusion-weighted imaging. Eighteen DLB subjects also underwent [^{11}C]-PK11195 PET imaging and 15 had [^{11}C]-Pittsburgh compound B amyloid PET, resulting in 9/15 being amyloid-positive. We used Computational Anatomy Toolbox (CAT12) for volume-based morphometry (VBM) and Tract-Based Spatial Statistics (TBSS) for DTI to assess group comparisons between DLB and controls and to identify associations of [^{11}C]-PK11195 binding with grey/white matter changes and cognitive score in DLB patients. VBM analyses showed that DLB had extensive reduction of grey matter volume in superior frontal, temporal, parietal and occipital cortices (family-wise error (FWE)-corrected $p < 0.05$). TBSS showed widespread changes in DLB for all DTI parameters (reduced fractional anisotropy, increased diffusivity), involving the corpus callosum, corona radiata and superior longitudinal fasciculus (FWE-corrected $p < 0.05$). Higher [^{11}C]-PK11195 binding in parietal cortices correlated with widespread lower mean and radial diffusivity in DLB patients (FWE-corrected $p < 0.05$). Furthermore, preserved cognition in DLB (higher Addenbrookes Cognitive Evaluation revised score) also correlated with higher [^{11}C]-PK11195 binding in frontal, temporal, and occipital lobes. However, microglial activation was not significantly associated with grey matter changes. Our study suggests that increased microglial activation is associated with a relative preservation of white matter and cognition in DLB, positioning neuroinflammation as a potential early marker of DLB etio-pathogenesis.

1. Introduction

Dementia with Lewy bodies (DLB) is the second-leading degenerative dementia in older people (Vann Jones and O'Brien, 2014). It is characterized by alpha-synuclein protein deposition in the form of intra-neuronal Lewy bodies as well as Lewy neurites, with a variable degree of concurrent Alzheimer's disease (AD) pathology (Spillantini et al., 1997; Gomperts, 2016). Neuroinflammation and,

* Corresponding author at: Department of Psychiatry, University of Cambridge School of Clinical Medicine, Box 189, Level E4 Cambridge Biomedical Campus, Cambridge CB2 0SP, United Kingdom.
E-mail address: john.obrien@medschl.cam.ac.uk (J.T. O'Brien).
[1] These authors contributed equally to the present work.
[2] Co-Senior Authors.

https://doi.org/10.1016/j.nicl.2020.102200
Received 30 October 2019; Received in revised form 26 January 2020; Accepted 27 January 2020
Available online 28 January 2020

more specifically microglial activation, is increasingly recognized as a key etio-pathogenic mechanism in DLB which can be assessed in vivo via different PET tracers including [^{11}C]-PK11195 (PK11195) (Turkheimer et al., 2007). In DLB, increased microglial activation as assessed via PK11195 has been observed in the striatum, substantia nigra, and several cortical regions (Iannaccone et al., 2013; Surendranathan et al., 2018). Intriguingly, we have recently found that patients with cognitively mild forms of DLB have higher PK11195 binding than those with moderate cognitive impairment in the caudate, thalamus as well as frontal, temporal, and parietal cortices (Surendranathan et al., 2018). Other studies have also shown that microglial activation is an initial event in AD, mirroring the neuropathological changes primarily involving temporo-parietal regions (Hamelin et al., 2016; Passamonti et al., 2018). In addition, longitudinal data regarding neuroinflammation activation in mild cognitive impairment (MCI) have shown a decreased microglial activation at 14-month follow-up (Fan et al., 2017). Increased microglial activation in MCI was also associated with a preserved hippocampal volume (Femminella et al., 2019). Together, these results suggest that neuroinflammation represents an early event in the neurodegeneration process and could be a potential therapeutic target in dementia. In fact, unlike molecules targeting protein accumulation which are currently at an experimental stage, anti-inflammatory drugs are readily available and could be employed more quickly into clinical drug trials. An important prerequisite for such an endeavour is a better understanding of the temporal ordering and clinical relevance of protein accumulation, neuroinflammation, and structural brain changes.

White matter microstructure has received growing research attention as a sensitive marker for early structural brain changes. Diffusion-tensor imaging (DTI) is sensitive to Brownian motion of water molecules, from which microstructural features and associated pathological processes can be inferred from the relative coherence or magnitude of diffusion along the major axis of a white matter bundle. Fractional anisotropy (FA) is a scalar index (range: 0–1) reflecting the directional coherence of water diffusion. Mean diffusivity (MD) represents the overall magnitude of diffusion and is widely thought to be sensitive to cell loss, cellularity, edema and necrosis (Pierpaoli and Basser, 1996; Alexander et al., 2007). A less commonly studied marker is radial diffusivity (RD), which has been linked to demyelination as well as pathological changes in axonal density (Klawiter et al., 2011). The literature has consistently shown reduced FA and increased MD/RD in DLB, especially in the absence of the marked brain atrophy that is typically seen in late-onset AD (Kantarci et al., 2010; Watson et al., 2012; Nedelska et al., 2015). Several pathological mechanisms for such white matter changes have been described in dementia, including ischaemia, demyelination and amyoid angiopathy (Gold et al., 2012; Chao et al., 2013; Kantarci et al., 2017). In addition to white matter changes secondary to grey matter atrophy and amyloid burden (i.e. Wallerian degeneration) (Amlien and Fjell, 2014), several other contributors such as vascular damage and tau deposition can contribute to primary white matter changes, especially in late-myelinated projection fibers (Bartzokis et al., 2007).

In the present study, we aimed to characterize the relationship between microglial activation as measured with PK11195 PET and DTI impairment in a cross-sectional group of subjects with probable DLB, most of which having amyloid status additionally confirmed through PiB PET imaging (Surendranathan et al., 2018). We recently observed that DLB subjects with a milder cognitive impairment had widespread higher cortical PK11195 binding. In addition, recent studies in MCI suggest an early peak of microglial activation in MCI. Therefore, we hypothesized that higher microglial activation would correlate with a relative preservation of white matter microstructural integrity.

2. Methods

2.1. Participants

The present work is part of the Neuroimaging of Inflammation in MemoRy and Other Disorders (NIMROD) study (Bevan-Jones et al., 2017). All participants were aged over 50 years and had sufficient proficiency in English for cognitive testing. We included 19 participants with probable DLB according to both 2005 and 2017 consensus criteria (McKeith et al., 2005; McKeith et al., 2017) as described in (Surendranathan et al., 2018). In addition, subjects had at least two years clinical follow-up to confirm clinical progression and no change of diagnosis. We also recruited 20 similarly aged healthy controls, with MMSE scores greater than 26, absence of regular memory complaints, and no unstable or significant medical illnesses. A detailed clinical and neuropsychological assessment was performed (Bevan-Jones et al., 2017). This included Addenbrooke's Cognitive Examination Revised test (ACE-R) which is a 100-point test incorporating five key cognitive domains in dementia disorders (orientation/attention, memory, verbal fluency, language, and visuo-spatial) (Mioshi et al., 2006).

Patients were identified from the Memory clinic at the Cambridge University Hospitals NHS Trust, other local memory clinics, and from the Dementias and Neurodegenerative Diseases Research Network (DeNDRoN) volunteer registers. Healthy controls were recruited via DeNDRoN as well as from spouses and partners of participants. Informed written consent was obtained in accordance with the Declaration of Helsinki. The study received a favourable opinion from the East of England Ethics Committee (Cambridge Central Research, Ref. 13/EE/0104).

2.2. MRI and PET acquisition

Nineteen subjects with probable DLB underwent multi-modal 3T MPRAGE and diffusion-weighted imaging (DWI) as described in detail below. 18/19 DLB participants also had [^{11}C]-PK11195 PET imaging on a GE Advance or GE Discovery 690 PET/CT scanner. To ensure accurate correlations between MRI and PET imaging, we aimed at keeping scan interval between MRI and PET within 3 months (mean interval 2.4 months). Each [^{11}C]-PK11195 PET image series was aligned across the time frames with SPM12 to ameliorate the impact of head motion during data acquisition. The realigned dynamic PET images were co-registered to the corresponding T1-weighted MPRAGE images, as were regions of interest (ROIs) from the Hammers atlas (Hammers et al., 2003) using ANTs for the inverse spatial normalisation from MNI to MPRAGE space. Prior to kinetic modelling, regional time-activity curves (TACs) were corrected for CSF contamination through division by the mean ROI fraction of grey plus white matter, using SPM12 tissue probability maps smoothed to PET spatial resolution. Binding in each ROI was quantified using non-displaceable binding potential (BP_{ND}) determined with reference tissue TAC estimation from supervised cluster analysis and a simplified reference tissue model incorporating vascular binding correction (Yaqub et al., 2012). In fact, the partial volume correction method applied to the dynamic PK11195 images to address differential atrophy is the two-compartment (brain, CSF) Meltzer method, which has been shown to be more robust to registration and segmentation errors than the three-compartment version. Furthermore, this method is well suited to the production of the PK11195 reference time activity curve from supervised cluster analysis (SCA), whereas the geometric transfer matrix (GTM) approach cannot be applied given that SCA is a voxel-wise technique.

For each subject, we derived a composite PK11195 BP_{ND} (global) by averaging the PK11195 binding across each cortical ROI and hemisphere from the Hammers atlas, as well as lobar PK11195 BP_{ND} (i.e., frontal, temporal, parietal, occipital). In addition, 15 DLB subjects underwent [^{11}C]-PiB PET imaging to quantify the density of fibrillar Aβ deposits for classification of Aβ status (positive when PiB cortical

standardized uptake value ratio (SUVR) > 1.5) (Jagust et al., 2010). [^{11}C]-PiB data were quantified using SUVR with the superior cerebellar grey matter as the reference region. The [^{11}C]-PiB SUVR data were subjected to the GTM technique using Freesurfer's PETsurfer (Greve et al., 2014), including partial volume correction.

2.3. Diffusion-weighted imaging

The DWI acquisition protocol was as follows: 63 slices of 2.0 mm thickness, TE = 106 ms, TR = 11,700 ms, SENSE = 2, field of view = 192 × 192 mm^2. The data were preprocessed with the FSL 5.0 software package (http://www.fmrib.ox.ac.uk/fsl). This included registration of all diffusion-weighted images to the b = 0 (i.e. no diffusion) volume using the FSL Diffusion Toolbox (*FDT*), followed by brain masks creation with *Brain Extraction Tool* (*BET*), head movement and eddy currents correction. We then used *DTIfit* to independently fit the diffusion tensor for each voxel, resulting in the derivation of FA, MD and RD.

2.4. Volume-based morphometry

In addition, volume-based morphometry (VBM) analyses were performed using high-resolution T1-weighted MPRAGE images, including group comparisons between DLB and Controls, as well as voxel-wise correlational grey matter maps of global/lobar PK11195 binding, in order to assess whether grey matter atrophy/preservation was significantly associated with increased microglial activation. Computational Anatomy Toolbox 12 (CAT12) was used to create 8mm-smoothed VBM maps, after using the standard CAT12 pipeline previously described in Nicastro et al. (2019).

2.5. Statistical analyses

Tract-based spatial statistics (*TBSS*) was implemented in the FSL workspace to align each subject's FA image to a pre-identified target FA image (FMRIB_58) (Smith et al., 2004). All aligned FA images were then affine-registered into the Montreal Neurological Institute (MNI) MNI152 template. The mean FA and skeleton were created for all subjects and each FA image was then projected onto the skeleton. The skeleton was thresholded at FA value of 0.2 to include white matter tracts that are common across all subjects, as well as to further exclude voxels that may contain grey matter or CSF. The aligned DTI parameter map of each subject was then projected onto the mean skeleton. In addition, other DTI parameters were aligned by applying the original FA non-linear spatial transformations to the corresponding datasets and projecting them onto the mean FA skeleton. Subsequently, the *randomise* function in FSL was implemented to identify group differences in DTI parameters between DLB and age-matched healthy controls, using a two-sample t-test while controlling for age and sex. VBM group comparisons between DLB and Controls were performed using the TFCE toolbox with non-parametric randomisation (n = 5000 permutations) and family-wise error (FWE)-corrected two-tailed $p < 0.05$ threshold, with age, sex and total intracranial volume as covariates.

Voxel-wise correlation between DTI and PK11195 was performed with TBSS using age, sex, scan interval between MRI and PET imaging, as well as ACER score as nuisance covariates in the design matrix. Global and lobar PK11195 uptake was treated as the independent variable for each DTI parameter across the white matter skeleton. The statistical significance from these tests was determined using non-parametric permutation testing (n = 5000 permutations) and adjusted for multiple comparisons FWE correction and using two-tailed $p < 0.05$ significance threshold (Smith and Nichols, 2009), thus obviating the need to set an arbitrary cluster threshold. Anatomical definitions of significant TBSS clusters were performed visually and facilitated using the John Hopkins – ICBM white matter atlas, available as part of the FSL package. Finally, the statistical maps were dilated with tbss_fill function for visualisation purposes. Similarly, voxelwise VBM correlational maps with global/lobar PK11195 were obtained for DLB subjects, using the same covariates as for DTI correlations (in addition to total intracranial volume). False-discovery rate (FDR) $p < 0.05$ was used as a significance threshold.

Table 1
Clinical characteristics of study sample.

	DLB (n = 19)	HC (n = 20)	p-value
Age *(years)*	73.5 ± 6.1 (62–82)	71.0 ± 6.9 (56–81)	0.23 *
Male/Female Ratio	3.8 (15/4)	1 (10/10)	0.06 $
Education *(years)*	12.0 ± 2.3 (8–17)	13.4 ± 2.8 (9–19)	0.10 *
MMSE	22.5 ± 4.3 (15–28)	28.8 ± 1.2 (26–30)	<0.0001 #
ACER	66.8 ± 11.9 (45–87)	90.9 ± 6.6 (75–100)	<0.0001 #

Abbreviations: M/F = Male/Female, MMSE = Mini-Mental State Examination, ACER = Addenbrooke's Cognitive Evaluation Revised, * = t-test, # = Mann-Whitney, $ = Chi-Square test.

3. Results

3.1. Demographics

The demographics and clinical characteristics are reported in **Table 1**. Both groups were comparable in terms of age, sex and years of education. As expected, MMSE and ACER scores were significantly lower in the DLB group relative to the healthy controls ($p < 0.001$, *Mann-Whitney U test*).

3.2. Group comparisons of DTI/VBM parameters

Voxel-based TBSS analyses revealed that the DLB group relative to controls had significant white matter changes in the body and splenium of corpus callosum. These findings were consistently observed for all three DTI metrics (decreased FA, increased MD and RD). In addition, we observed reduced FA and increased RD for DLB in right anterior and posterior corona radiata, left cingulate gyrus, and right superior longitudinal fasciculus (Fig. 1) (all FWE-corrected $p < 0.05$).

Subgroup analyses of DLB subjects according to their PiB status revealed a more extensive impairment in the PiB+ DLB (n = 9) compared to controls, with virtually every subcortical tract being impaired. In contrast, there was no significant DTI changes in the PiB- DLB subgroup (n = 6) compared to controls. DTI group comparisons between PiB+ (n = 9) and PiB- DLB (n = 6) did not show any significant cluster (all FWE-corrected $p > 0.17$).

VBM group comparisons showed that, in comparison to Controls, DLB subjects had lower grey matter volume in regions including bilateral superior and middle frontal, middle and posterior temporal, inferior parietal and lateral occipital cortices (FWE-corrected $p < 0.05$, Fig. 2).

3.3. PK11195 binding in DLB

As previously shown with the same DLB group (Surendranathan et al., 2018), PK11195 PET comparisons with a similarly-aged control group showed that DLB subjects had higher PK11195 binding in the fusiform gyrus and putamen ($p < 0.01$, *Mann-Whitney U test*). Using a median-split approach to dichotomise DLB subjects into a mild cognitive impairment subgroup (ACER score >65/100) and a moderate-severe cognitive impairment subgroup (ACER score ≤65/100) revealed that the "mild" DLB group had higher PK11195 binding than Controls in the inferior and medial temporal gyrus, fusiform gyrus, putamen, inferior frontal gyrus and cuneus. Conversely, there was no significant difference between the moderate-severe DLB subgroup and Controls, except for a higher PK11195 in the caudate nucleus for the Control group (details available in

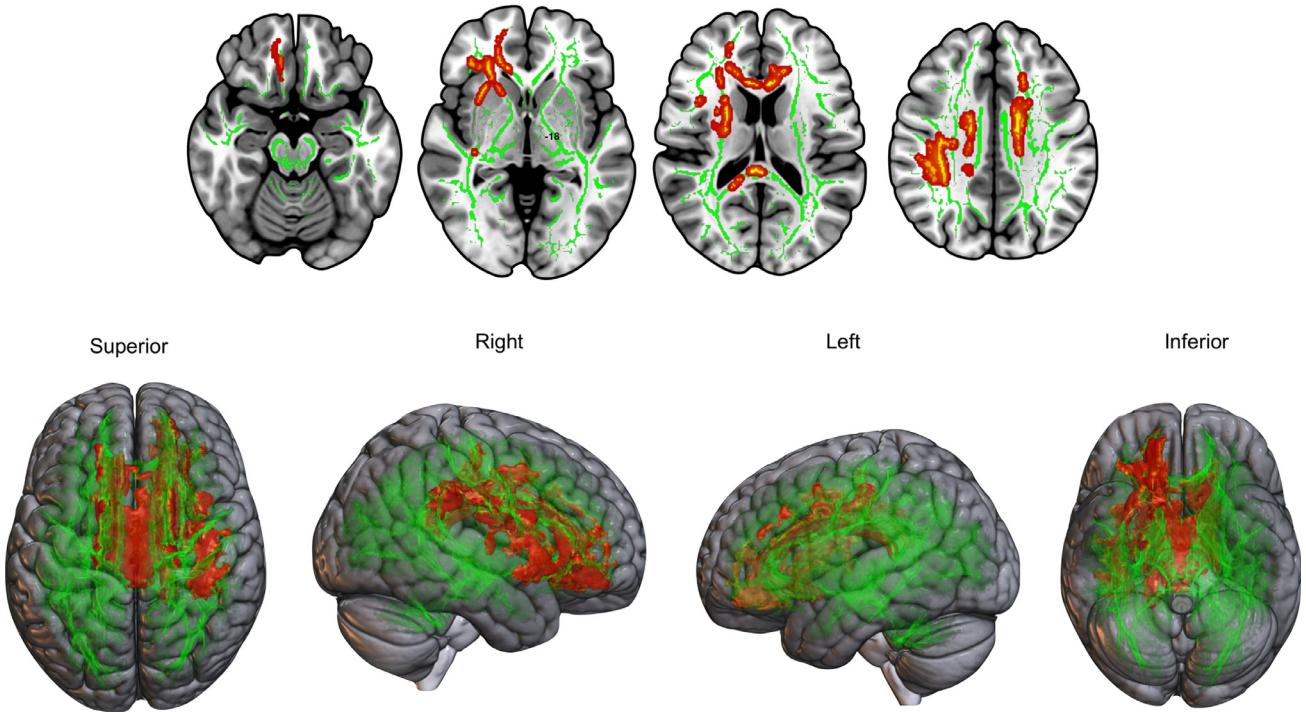

Fig. 1. DTI group comparisons showing increased radial diffusivity (red) in DLB subjects compared to healthy control group (FWE $p < 0.05$). (For interpretation of the references to color in this figure legend, the reader is referred to the web version of this article.)

(Surendranathan et al., 2018)). In addition, we observed that DLB subjects had lower BP_{ND} in the parietal lobe (0.03 ± 0.06) compared to the frontal (0.10 ± 0.08, $p = 0.008$) and occipital lobes (0.11 ± 0.08, $p = 0.002$, *Mann-Whitney U test*).

Higher ACER score was significantly correlated with higher PK11195 binding in frontal (Spearman ρ = 0.52, $p = 0.03$, 95% CI 0.137 – 0.91), temporal (ρ = 0.50, $p = 0.03$, 95% CI 0.128–0.878) and occipital lobe (ρ = 0.55, $p = 0.02$, 95% CI 0.209–0.898), with a trend for global PK (ρ = 0.46, $p = 0.052$, 95% CI 0.094–0.834) but not with parietal PK binding (ρ = 0.26, $p = 0.23$, 95% CI −0.185–0.741).

3.4. Voxel-wise association of imaging data

TBSS analyses revealed that for DLB subjects, higher parietal PK11195 uptake was associated with a relative preservation of white matter (i.e., lower MD and RD) in bilateral corona radiata, posterior thalamic radiations, sagittal stratum, left superior longitudinal fasciculus, as well as frontal and parietooccipital white matter tracts (two-tailed FWE $p < 0.05$) (Fig. 3). We did not find significant associations between PK11195 and FA ($p = 0.05$), nor were there any significant correlations in the opposite contrasts for MD and RD.

PK11195 – DTI correlation analyses did not reach a significant threshold regarding PK11195 at the global (all $p > 0.13$), frontal (all $p > 0.13$), temporal (all $p > 0.08$) and occipital level (all $p > 0.13$) (all voxelwise FWE-corrected).

Regarding voxelwise correlations between DTI and lobar/global amyloid load in the subset of DLB subjects with available PiB PET ($n = 15$), these analyses did not reach statistical significance (all FWE-corrected $p > 0.3$).

In addition, no significant correlation was observed in the DLB group between VBM maps and global/lobar (increased or decreased) PK11195 binding (all FDR-corrected $p > 0.3$).

4. Discussion

In the present study, we found evidence of relative DTI preservation for DLB in relation to increased microglial activation as measured with PK11195. This is consistent with our previous data showing that neuroinflammation in fronto-temporo-parietal cortices was more prominent in DLB subjects with milder cognitive impairment, suggesting that central inflammation plays a pivotal role in the early stages of the disease (Surendranathan et al., 2018). No such correlation (either negative or positive) was observed between grey matter volume and PK11195 binding - microglial activation does not decrease in relation to

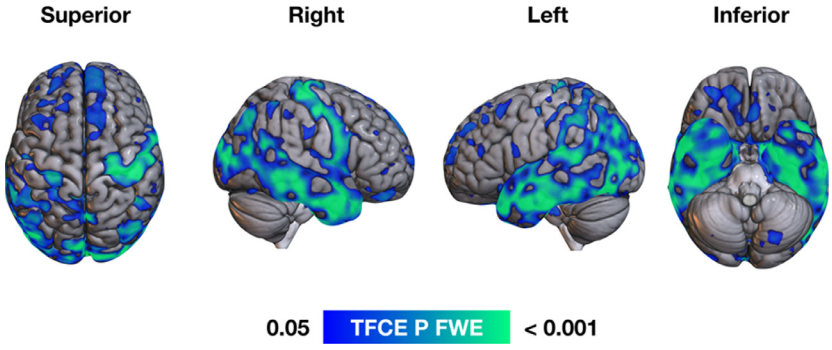

Fig. 2. VBM group comparisons showing reduced grey matter volume (blue-green) for DLB subjects in bilateral superior frontal, medial, lateral and posterior temporal, parietal and lateral occipital cortices (FWE $p < 0.05$). (For interpretation of the references to color in this figure legend, the reader is referred to the web version of this article.)

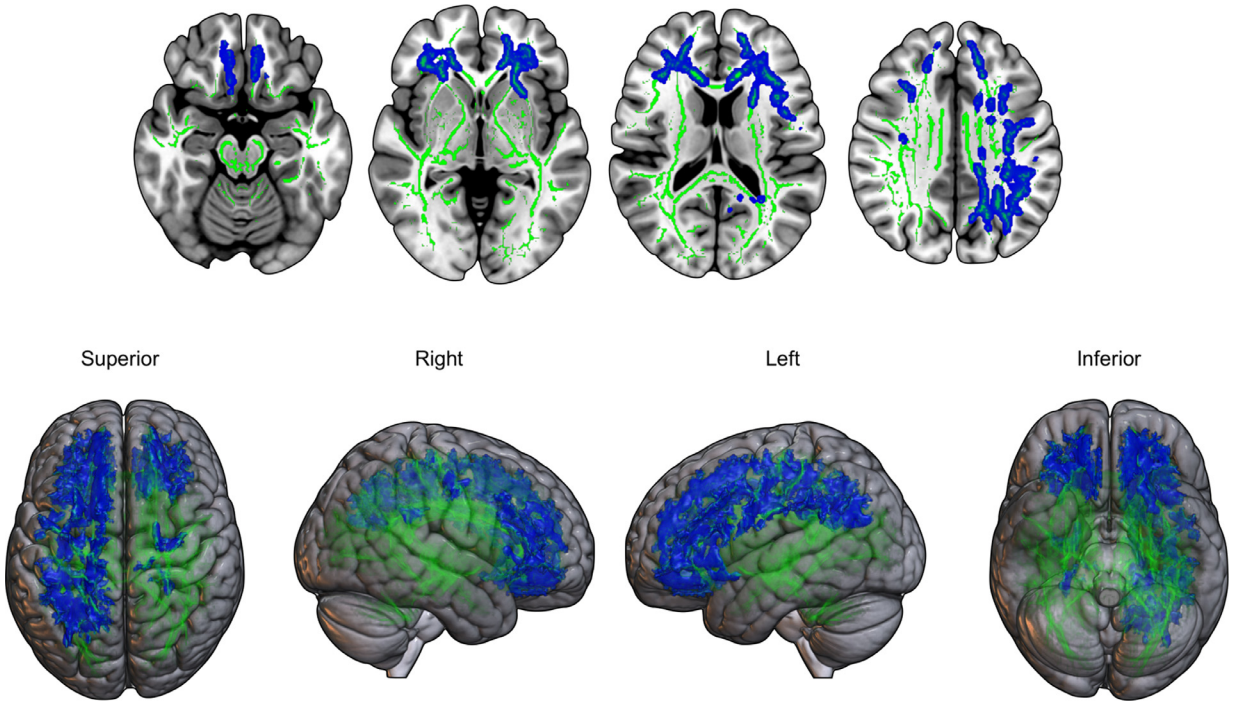

Fig. 3. TBSS correlation analyses showing decreased radial diffusivity (blue) correlated with higher parietal ^{11}C-PK11195 binding in DLB subjects (FWE $p < 0.05$). (For interpretation of the references to color in this figure legend, the reader is referred to the web version of this article.)

grey matter atrophy and conversely, increased neuroinflammation is not directly related to preserved grey matter volume.

Extensive grey and white matter abnormalities were observed in DLB compared to healthy controls. Patients exhibited grey matter atrophy in extensive frontal, temporal, parietal and occipital cortices (Fig. 2), while DTI changes were observed in the corpus callosum, corona radiata, superior longitudinal fasciculus and left cingulum (Fig. 1), which is in keeping with previous studies (Firbank et al., 2007; Kantarci et al., 2010; Watson et al., 2012; Delli Pizzi et al., 2015; Firbank et al., 2016). Subgroup analyses according to the PiB status showed that PiB + DLB subjects had more extensive DTI changes, encompassing virtually every tract of the white matter skeleton. Most likely due to a small sample size, we did not find any significant DTI difference between PiB + and PiB- DLB subjects. Interestingly, previous studies showed altered DTI metrics in parietal and occipital white matter tracts in DLB, irrespective of the amyloid load (Nedelska et al., 2015).

Studies in AD report that white matter changes can occur secondarily to grey matter damage (Wallerian degeneration) (Amlien and Fjell, 2014) following amyloid accumulation in soluble oligomers or plaques. Cell death will lead to axonal disruption in white matter tracts connecting the affected cortical areas. However, there is also evidence of primary white matter changes, which can be attributed to vascular damage or hyperphosphorylated tau deposition, resulting in the formation of paired helical filaments primarily affecting the axons. The retrogenesis hypothesis stipulates that primary white matter degeneration follows an inverse path than what is observed during myelogenesis, i.e., early-myelinated large-diameter fibres are affected last, while late-myelinated projecting fibres shown early disruption (Bartzokis et al., 2007). Longitudinal DTI studies accounting for tau deposition and vascular burden are warranted to disentangle primary and secondary white matter changes in dementias.

In the present study, we also observed that higher parietal PK11195 binding was correlated with relative DTI preservation (i.e., lower diffusivity) in the corona radiata and superior longitudinal fasciculus, i.e., the same tracts which are impaired in DLB compared to controls (Fig. 3). Thus, the spatial congruence of both statistical maps – subjected to the same rigorous statistical thresholds – confer support for the view that white matter deficits may be a secondary event to various processes such as protein deposition and possibly neuroinflammation. In addition, we observed a broad overlap between the findings of MD and RD parameters regarding the correlation of DTI values and PK11195 binding. Higher MD values indicate increased diffusion, suggesting tissue breakdown and increased brain water content. Conversely, higher RD is considered as a more specific marker of myelin damage (Pierpaoli and Basser, 1996; Song et al., 2005). As previously reported, MD (and RD) appears as a more sensitive proxy of white matter damage than FA in patients with DLB (Watson et al., 2012; O'Donovan et al., 2014; Delli Pizzi et al., 2015).

Whereas lower MD and RD DTI values are related to higher parietal PK11195, the analyses did not reach statistical significance for PK11195 binding in the other lobes, although we observed a trend for temporal lobe ($p > 0.08$). Considering this is a cross-sectional study, one could only speculate about the reasons why parietal PK11195 is more closely related to DTI preservation than the other brain regions. We can hypothesize that the dynamic changes in parietal PK11195 are temporally more related to DTI changes, possibly as parietal PK11195 is decreasing simultaneously with appearing white matter changes. In fact, we observed that PK11195 binding in the parietal lobe was significantly lower compared to the frontal and occipital lobes.

Studies using TSPO PET ligands in degenerative conditions have reported conflicting results about the trajectory of microglial activation. One hypothesis suggests that neuroinflammation is more prominent at earlier stages of degenerative conditions. In fact, Femminella et al. (Femminella et al., 2019) showed that increased microglial activation as measured with [^{11}C]-PBR28 PET in MCI subjects was associated with higher grey matter and hippocampal volume. Similarly, Hamelin et al. (Hamelin et al., 2016) observed that higher TSPO binding (using ^{18}F-DPA-714) was positively correlated with higher MMSE and larger grey matter volume in AD. Moreover, a recent study in a transgenic amyloid mouse model (Blume et al., 2018) using longitudinal TSPO and amyloid PET showed that microglial response declined relative to increasing amyloidosis, possibly due to a saturation effect. Interestingly, while our results suggest that increased TSPO binding is directly related to lower

diffusivity, no such relationship could be established between PK11195 binding and grey matter volume. These findings are crucial as they suggest that decreased microglial activation with progressive impairment of DTI metrics and cognition is not secondary to grey matter atrophy.

As discussed in a recent meta-analysis (Bradburn et al., 2019), the predominant hypothesis posits that neuroinflammation peaks early in MCI, followed by a second peak when MCI convert to AD, possibly reflecting the complex relationship between microglial activation and protein deposition internalized by glia (Fan et al., 2017). Therefore, our observations in DLB suggest a different pattern of microglial activation in dementias compared to primary inflammatory conditions, where TSPO ligand changes are more related to clinical relapses, as this is the case in multiple sclerosis (Rissanen et al., 2018).

Regarding the relationship between amyloid load and PK11195 binding, we did not observe any significant correlation between lobar or global PiB SUVR and PK11195 BP_{ND}, suggesting that amyloid load is not a major driver of neuroinflammation in DLB, or that any such relationship is weak. These findings are in contrast with those observed in AD (Fan et al., 2015).

The present study is not without limitations. First, our results have been obtained on a relatively modest sample of subjects with DLB, so this would require confirmation in larger samples, especially since we found a trend between higher microglial activation in the temporal lobe and DTI preservation. In addition, while subgroup analyses based on the amyloid status would certainly be of interest, our small sample impeded us to assess whether concurrent AD pathology might play an additional role in the complex relationship between neuroinflammation and white matter tracts integrity. Second, the present study was based on data obtained with a cross-sectional design. Therefore, longitudinal data is required to fully assess the spatial and temporal interplay between white matter integrity and neuroinflammation in DLB. If on the one hand, white matter degeneration can be considered as an early structural marker in neurodegenerative disorders, it can be equally possible that neuroinflammation precipitates white matter damage and thus represents a relatively “upstream” event in the cascade leading to cellular loss in DLB. In addition, we must acknowledge that there was a larger male distribution in the DLB group (15/19 versus 10/20 for Controls, $p = 0.06$) and although we used sex as a covariate for our correlational analyses, we cannot exclude that sex might play a role in DTI integrity. In fact, Kumar et al. showed that females had a lower myelin and fiber integrity in limbic and cerebellar regions, while males had lower values in frontal and temporal areas (Kumar et al., 2013). Additionally, we are not aware of a different microglial activation based on sex.

The use of PK11195 targeting translocator protein (TSPO) cannot fully represent the extent of central inflammation which is determined by several other factors over and above microglial activation. In fact, other targets such as astrocyte activation should be assessed as they also may play a role in the development of neurodegeneration (Stefaniak and O'Brien, 2016). In addition, PK11195, as a first generation TSPO ligand, has shown lower sensitivity compared to second generation tracers. However, PK11195 has the advantage of not being affected by the genetic polymorphism (notably rs6971 single nucleotide) altering the binding of second-generation ligands (Owen et al., 2012).

Finally, although TBSS is a widely used DTI analysis software, inherent limitations must be acknowledged, e.g. the fact that the projection of the common white matter skeleton is based on FA maps rather than tensor-based. In addition, the registration target was performed on the FMRIB58 skeleton (as recommended by FSL) rather than on a study-specific skeleton (Bach et al., 2014). In addition, we must acknowledge that the tensor model used in the present study does not address the issue of crossing fibres, which can represent 70% of the configuration of white matter fibres. More sophisticated models, including diffusion and fibre orientation density stand as a more effective way to describe the complex organisation of white matter tracts (Dell'Acqua and Tournier, 2019).

In conclusion, we present novel evidence of the in vivo association between lower DTI diffusivity and increased microglial activation in DLB. Future longitudinal studies are required to determine whether the early presence of neuroinflammation in DLB recedes and mediates the structural brain abnormalities that we have observed.

Ethical approval

The present study was performed in agreement with the Declaration of Helsinki and its further amendments. Approval was obtained from Ethics Committee from East of England (Cambridge Central Research, Ref. 13/EE/0104).

Informed consent

Informed consent has been obtained from all participants in the present study.

Funding

We thank Alzheimer Research UK for funding the ^{11}C-PK11195 PET imaging in DLB subjects, the Cambridge PD+ centre, the National Institute for Health Research Cambridge Biomedical Research Centre (NIHR, RG64473), the Wellcome Trust (JBR: 103838) and the Medical Research Council (FIA: MR/K02308X/1; LP: MR/P01271X/1) for funding and support.

CRediT authorship contribution statement

Nicolas Nicastro: Conceptualization, Methodology, Formal analysis, Software, Writing - original draft. **Elijah Mak:** Conceptualization, Methodology, Formal analysis, Software, Writing - original draft. **Guy B. Williams:** Investigation, Writing - review & editing. **Ajenthan Surendranathan:** Writing - review & editing. **W Richard Bevan-Jones:** Writing - review & editing. **Luca Passamonti:** Writing - review & editing. **Patricia Vàzquez Rodrìguez:** Writing - review & editing. **Li Su:** Writing - review & editing. **Robert Arnold:** Data curation, Writing - review & editing. **Tim D. Fryer:** Software, Writing - review & editing. **Young T. Hong:** Software, Writing - review & editing. **Franklin I. Aigbirhio:** Conceptualization, Funding acquisition, Writing - review & editing. **James B. Rowe:** Conceptualization, Methodology, Funding acquisition, Supervision, Writing - review & editing. **John T. O'Brien:** Conceptualization, Methodology, Funding acquisition, Supervision, Writing - review & editing.

Declaration of Competing Interest

N. Nicastro, E. Mak, G.B. Williams, A. Surendranathan, W.R. Bevan-Jones, L. Passamonti, Robert Arnold, Tim D. Fryer and Young T. Hong report no disclosures relevant to the present manuscript. F. I. Aigbirhio has served as review editor for *Journal of Labelled Compounds and Radiopharmaceuticals*, received academic grant support from GE Healthcare, and served as a consultant for Avid and Cantabio, all for matters not related to the current study. J. B. Rowe serves as editor to *Brain*, has been a consultant for Asceneuron and Syncona, and has received academic grant funding from AZ-MedImmune, Janssen, and Lilly, unrelated to this study. J. T. O'Brien has served as deputy editor of *International Psychogeriatrics*, received grant support from Avid (Lilly), and served as a consultant for Avid and GE Healthcare, all for matters not related to the current study.

Acknowledgements

We are grateful to our volunteers for their participation in the

NIMROD study. We thank the radiographers at Wolfson Brain Imaging Centre and the PET/CT unit, Addenbrooke's Hospital for their technical expertise and support in data acquisition. We thank the NIHR Dementias and Neurodegenerative Research Network for their help with subject recruitment. We also thank Dr Istvan Boros, Dr. Joong-Hyun Chun, and WBIC RPU for the manufacture of the [^{11}C]-PK11195.

References

Alexander, A.L., Lee, J.E., Lazar, M., Field, A.S, 2007. Diffusion tensor imaging of the brain. Neurotherapeutics 4 (3), 316–329.
Amlien, I.K., Fjell, A.M., 2014. Diffusion tensor imaging of white matter degeneration in Alzheimer's disease and mild cognitive impairment. Neuroscience 276, 206–215.
Bach, M., Laun, F.B., Leemans, A., Tax, C.M., Biessels, G.J., Stieltjes, B., et al., 2014. Methodological considerations on tract-based spatial statistics (TBSS). Neuroimage 100, 358–369.
Bartzokis, G., Lu, P.H., Mintz, J, 2007. Human brain myelination and amyloid beta deposition in Alzheimer's disease. Alzheimers Dement. 3 (2), 122–125.
Bevan-Jones, W.R., Surendranathan, A., Passamonti, L., Vazquez Rodriguez, P., Arnold, R., Mak, E., et al., 2017. Neuroimaging of inflammation in memory and related other disorders (NIMROD) study protocol: a deep phenotyping cohort study of the role of brain inflammation in dementia, depression and other neurological illnesses. BMJ Open 7 (1), e013187.
Blume, T., Focke, C., Peters, F., Deussing, M., Albert, N.L., Lindner, S., et al., 2018. Microglial response to increasing amyloid load saturates with aging: a longitudinal dual tracer in vivo muPET-study. J. Neuroinflammation 15 (1), 307.
Bradburn, S., Murgatroyd, C., Ray, N., 2019. Neuroinflammation in mild cognitive impairment and alzheimer's disease: a meta-analysis. Ageing Res. Rev. 50, 1–8.
Chao, L.L., Decarli, C., Kriger, S., Truran, D., Zhang, Y., Laxamana, J., et al., 2013. Associations between white matter hyperintensities and beta amyloid on integrity of projection, association, and limbic fiber tracts measured with diffusion tensor MRI. PLoS ONE 8 (6), e65175.
Dell'Acqua, F., Tournier, J.D., 2019. Modelling white matter with spherical deconvolution: how and why? NMR Biomed. 32 (4), e3945.
Delli Pizzi, S., Franciotti, R., Taylor, J.P., Esposito, R., Tartaro, A., Thomas, A., et al., 2015. Structural connectivity is differently altered in dementia with Lewy body and Alzheimer's disease. Front. Aging Neurosci. 7, 208.
Fan, Z., Brooks, D.J., Okello, A., Edison, P, 2017. An early and late peak in microglial activation in Alzheimer's disease trajectory. Brain 140 (3), 792–803.
Fan, Z., Okello, A.A., Brooks, D.J., Edison, P, 2015. Longitudinal influence of microglial activation and amyloid on neuronal function in Alzheimer's disease. Brain 138 (Pt 12), 3685–3698.
Femminella, G.D., Dani, M., Wood, M., Fan, Z., Calsolaro, V., Atkinson, R., et al., 2019. Microglial activation in early Alzheimer trajectory is associated with higher gray matter volume. Neurology 92 (12), e1331–e1343.
Firbank, M.J., Blamire, A.M., Krishnan, M.S., Teodorczuk, A., English, P., Gholkar, A., et al., 2007. Diffusion tensor imaging in dementia with Lewy bodies and Alzheimer's disease. Psychiatry Res. 155 (2), 135–145.
Firbank, M.J., Watson, R., Mak, E., Aribisala, B., Barber, R., Colloby, S.J., et al., 2016. Longitudinal diffusion tensor imaging in dementia with Lewy bodies and Alzheimer's disease. Parkinsonism Relat. Disord. 24, 76–80.
Gold, B.T., Johnson, N.F., Powell, D.K., Smith, C.D, 2012. White matter integrity and vulnerability to Alzheimer's disease: preliminary findings and future directions. Biochim. Biophys. Acta 1822 (3), 416–422.
Gomperts, S.N., 2016. Lewy body dementias: dementia with Lewy bodies and Parkinson disease dementia. Continuum (Minneap Minn) 22 (2 Dementia), 435–463.
Greve, D.N., Svarer, C., Fisher, P.M., Feng, L., Hansen, A.E., Baare, W., et al., 2014. Cortical surface-based analysis reduces bias and variance in kinetic modeling of brain PET data. Neuroimage 92, 225–236.
Hamelin, L., Lagarde, J., Dorothee, G., Leroy, C., Labit, M., Comley, R.A., et al., 2016. Early and protective microglial activation in Alzheimer's disease: a prospective study using 18F-DPA-714 PET imaging. Brain 139 (Pt 4), 1252–1264.
Hammers, A., Allom, R., Koepp, M.J., Free, S.L., Myers, R., Lemieux, L., et al., 2003. Three-dimensional maximum probability atlas of the human brain, with particular reference to the temporal lobe. Hum. Brain Mapp. 19 (4), 224–247.
Iannaccone, S., Cerami, C., Alessio, M., Garibotto, V., Panzacchi, A., Olivieri, S., et al., 2013. In vivo microglia activation in very early dementia with Lewy bodies, comparison with Parkinson's disease. Parkinsonism Relat. Disord. 19 (1), 47–52.
Jagust, W.J., Bandy, D., Chen, K., Foster, N.L., Landau, S.M., Mathis, C.A., et al., 2010. The Alzheimer's disease neuroimaging initiative positron emission tomography core. Alzheimers Dement. 6 (3), 221–229.
Kantarci, K., Avula, R., Senjem, M.L., Samikoglu, A.R., Zhang, B., Weigand, S.D., et al., 2010. Dementia with Lewy bodies and Alzheimer disease: neurodegenerative patterns characterized by DTI. Neurology 74 (22), 1814–1821.
Kantarci, K., Murray, M.E., Schwarz, C.G., Reid, R.I., Przybelski, S.A., Lesnick, T., et al., 2017. White-matter integrity on DTI and the pathologic staging of Alzheimer's disease. Neurobiol. Aging 56, 172–179.
Klawiter, E.C., Schmidt, R.E., Trinkaus, K., Liang, H.F., Budde, M.D., Naismith, R.T., et al., 2011. Radial diffusivity predicts demyelination in ex vivo multiple sclerosis spinal cords. Neuroimage 55 (4), 1454–1460.
Kumar, R., Chavez, A.S., Macey, P.M., Woo, M.A., Harper, R.M, 2013. Brain axial and radial diffusivity changes with age and gender in healthy adults. Brain Res. 1512, 22–36.
McKeith, I.G., Boeve, B.F., Dickson, D.W., Halliday, G., Taylor, J.P., Weintraub, D., et al., 2017. Diagnosis and management of dementia with Lewy bodies: fourth consensus report of the DLB Consortium. Neurology 89 (1), 88–100.
McKeith, I.G., Dickson, D.W., Lowe, J., Emre, M., O'Brien, J.T., Feldman, H., et al., 2005. Diagnosis and management of dementia with Lewy bodies: third report of the DLB Consortium. Neurology 65 (12), 1863–1872.
Mioshi, E., Dawson, K., Mitchell, J., Arnold, R., Hodges, J.R, 2006. The Addenbrooke's cognitive examination revised (ACE-R): a brief cognitive test battery for dementia screening. Int. J. Geriatr. Psychiatry 21 (11), 1078–1085.
Nedelska, Z., Schwarz, C.G., Boeve, B.F., Lowe, V.J., Reid, R.I., Przybelski, S.A., et al., 2015. White matter integrity in dementia with Lewy bodies: a voxel-based analysis of diffusion tensor imaging. Neurobiol. Aging 36 (6), 2010–2017.
Nicastro, N., Rodriguez, P.V., Malpetti, M., Bevan-Jones, W.R., Simon Jones, P., Passamonti, L., et al., 2019. (18)F-AV1451 PET imaging and multimodal MRI changes in progressive supranuclear palsy. J. Neurol (e-pub ahead of print).
O'Donovan, J., Watson, R., Colloby, S.J., Blamire, A.M., O'Brien, J.T, 2014. Assessment of regional MR diffusion changes in dementia with Lewy bodies and Alzheimer's disease. Int. Psychogeriatr. 26 (4), 627–635.
Owen, D.R., Yeo, A.J., Gunn, R.N., Song, K., Wadsworth, G., Lewis, A., et al., 2012. An 18-kDa translocator protein (TSPO) polymorphism explains differences in binding affinity of the PET radioligand PBR28. J. Cereb. Blood Flow Metab. 32 (1), 1–5.
Passamonti, L., Rodriguez, P.V., Hong, Y.T., Allinson, K.S.J., Bevan-Jones, W.R., Williamson, D., et al., 2018. [(11)C]PK11195 binding in Alzheimer disease and progressive supranuclear palsy. Neurology 90 (22), e1989–e1996.
Pierpaoli, C., Basser, P.J., 1996. Toward a quantitative assessment of diffusion anisotropy. Magn. Reson. Med. 36 (6), 893–906.
Rissanen, E., Tuisku, J., Vahlberg, T., Sucksdorff, M., Paavilainen, T., Parkkola, R., et al., 2018. Microglial activation, white matter tract damage, and disability in MS. Neurol. Neuroimmunol. Neuroinflamm. 5 (3), e443.
Smith, S.M., Jenkinson, M., Woolrich, M.W., Beckmann, C.F., Behrens, T.E., Johansen-Berg, H., et al., 2004. Advances in functional and structural MR image analysis and implementation as FSL. Neuroimage 23 (Suppl 1), S208–S219.
Smith, S.M., Nichols, T.E., 2009. Threshold-free cluster enhancement: addressing problems of smoothing, threshold dependence and localisation in cluster inference. Neuroimage 44 (1), 83–98.
Song, S.K., Yoshino, J., Le, T.Q., Lin, S.J., Sun, S.W., Cross, A.H., et al., 2005. Demyelination increases radial diffusivity in corpus callosum of mouse brain. Neuroimage 26 (1), 132–140.
Spillantini, M.G., Schmidt, M.L., Lee, V.M., Trojanowski, J.Q., Jakes, R., Goedert, M., 1997. Alpha-synuclein in Lewy bodies. Nature 388 (6645), 839–840.
Stefaniak, J., O'Brien, J., 2016. Imaging of neuroinflammation in dementia: a review. J. Neurol. Neurosurg. Psychiatr. 87 (1), 21–28.
Surendranathan, A., Su, L., Mak, E., Passamonti, L., Hong, Y.T., Arnold, R., et al., 2018. Early microglial activation and peripheral inflammation in dementia with Lewy bodies. Brain 141 (12), 3415–3427.
Turkheimer, F.E., Edison, P., Pavese, N., Roncaroli, F., Anderson, A.N., Hammers, A., et al., 2007. Reference and target region modeling of [11C]-(R)-PK11195 brain studies. J. Nucl. Med. 48 (1), 158–167.
Vann Jones, S.A., O'Brien, J.T, 2014. The prevalence and incidence of dementia with Lewy bodies: a systematic review of population and clinical studies. Psychol. Med. 44 (4), 673–683.
Watson, R., Blamire, A.M., Colloby, S.J., Wood, J.S., Barber, R., He, J., et al., 2012. Characterizing dementia with Lewy bodies by means of diffusion tensor imaging. Neurology 79 (9), 906–914.
Yaqub, M., van Berckel, B.N., Schuitemaker, A., Hinz, R., Turkheimer, F.E., Tomasi, G., et al., 2012. Optimization of supervised cluster analysis for extracting reference tissue input curves in (R)-[(11)C]PK11195 brain PET studies. J. Cereb. Blood Flow Metab. 32 (8), 1600–1608.